Journal of Organometallic Chemistry 897 (2019) 155–160

Contents lists available at ScienceDirect

Journal of Organometallic Chemistry

journal homepage: www.elsevier.com/locate/jorganchem

Synthesis, structure and dual-stimulus-responsive luminescence switching of a new platinum(II) complex based on 3-trimethylsilylethynyl-1,10-phenanthroline

Jiajia Kang, Jun Ni*, Yanqin Li, Jianjun Zhang

College of Chemistry, Dalian University of Technology, Linggong Road No. 2, Dalian, 116024, PR China

ARTICLE INFO

Article history:
Received 25 May 2019
Received in revised form
26 June 2019
Accepted 3 July 2019
Available online 4 July 2019

Keywords:
Platinum(II) complex
Dual-stimulu-responsive luminescence switching
Thermo-triggered luminescence switching
Mechanoluminescence
Pt-Pt contact

ABSTRACT

A new diimine-platinum(II) complex, Pt(PhenC≡CSiMe$_3$)(C≡C-C$_6$H$_4$-3-F)$_2$ (**1**) based on 3-trimethylsilylethynyl-1,10-phenanthroline (PhenC≡CSiMe$_3$), was synthesized and characterized. Two solvated crystals, **1**·1/2(ClCH$_2$CH$_2$Cl) and **1**·CHCl$_3$ exhibited dual-stimulus-responsive color and luminescence switching behaviors triggered by heating or mechanical grinding. Upon heating, the color and luminescence of both complexes were changed to red with luminescence red-shifting to 656 for **1**·1/2(ClCH$_2$CH$_2$Cl) and 691 nm for **1**·CHCl$_3$, corresponding to the thermo-triggered luminescence red-shifts of 112–142 nm and 156–189 nm, respectively. The different heated samples confirm that the original stacking structure can accurately affect the luminescence switching properties of luminescent switching materials. Under the mechanical grinding, both complexes were converted to the same red amorphous product with red emission peaked at 702 nm. Interestingly, once exposure to ClCH$_2$CH$_2$Cl or CHCl$_3$ vapor, the heated and ground samples could be thoroughly reverted to crystalline **1**·1/2(ClCH$_2$CH$_2$Cl) and **1**·CHCl$_3$. Such reversible thermo- and mechanical-grinding-triggered luminescence switching properties of the complexes are attributed to the interconversions of the lowest energy excited states between metal-to-ligand charge transfer (MLCT) and metal-metal-to-ligand charge transfer (MMLCT) transitions during the heating/grinding-vapor absorbing processes. Furthermore, **1**·CHCl$_3$ was successfully used for rewritable data recording.

1. Introduction

Luminescent switching materials (LSMs) that can change their color and luminescence under certain external stimuli have attracted considerable attention for their applications in various fields of environmental monitoring, medical treatment, sensor systems, information storage and security, display devices, energy regeneration and utilization, etc [1–16]. In the past two decades, the development of LSMs have made a great improvements. Many kinds of materials such as inorganic or nano-particles [17–21], organic compounds [22–25], metal complexes [26–29], and polymers [30–37] have been reported to possess the luminescence switching properties. Meanwhile, the mechanism of these luminescence switching properties have been deeply studied and clearly revealed.

In numerous LSMs, diimine-platinum(II) complex is the most special one due to its unique square-planar coordination geometry. First, square-planar platinum(II) complex allows close axial intimate interactions with other identical molecules to form dimer or aggregate species through Pt-Pt and/or π-π interactions, resulting in the red-shifted emission in both solution or solid states from triplet metal-metal to ligand charge transfer (^{3}MMLCT) [38–41]. Second, the rich and sensitive excited-state energy levels of platinum(II) complexes are easily perturbed by the conversion of stacking structures and intermolecular interactions derived from external stimuli, leading to their various luminescence switching behaviors [41–43]. Furthermore, luminescence switching behaviors of platinum(II) complexes usually exhibit higher sensitivity than other LSMs, enabled their better performance in the field of sensor system [44–47]. Although the luminescence switching properties based on platinum(II) complexes have been studied sufficiently, nevertheless, there still exist some unsolved problems. For example, up to now, we still can not predict the property of a new platinum(II) complex. We don't even know the role of stacking

* Corresponding author.
E-mail address: nijun@dlut.edu.cn (J. Ni).

https://doi.org/10.1016/j.jorganchem.2019.07.004
0022-328X/

structure played in luminescence switching property. Therefore, in-depth and systematic studies of LSMs are very important and necessary for better understanding and practical application of such materials.

Herein, we report the syntheses, structure, and the luminescence switching properties of a new diimine-platinum(II) complex based on 3-trimethylsilylethynyl-1,10-phenanthroline (PhenC≡C-$SiMe_3$) and 1-ethynyl-3-fluorobenzene ligands, namely Pt(PhenC≡C$SiMe_3$)(C≡C-C_6H_4-3-F)$_2$ (**1**) (Scheme 1). Two solvated crystalline forms, yellow-green **1**·1/2($ClCH_2CH_2Cl$) and yellow **1**·$CHCl_3$ were obtained. Upon heating or mechanical grinding, these species displayed drastic changes in both color and luminescence, resulting in their dual-stimulus-responsive luminescence switching properties. Systematic studies on the crystal structure, luminescence spectra, TGA, and PXRD indicated that the reversible luminescence switching properties of the complexes are due to interconversions of the lowest-energy excited states between MLCT (metal to ligand charge transfer) and MMLCT transitions. The mechanoluminescent switching property of them are caused by conversion of the molecular arrangement from crystalline to amorphous states and the formation of Pt-Pt interaction between adjacent molecules during the mechanical grinding. Furthermore, based on reversible mechanoluminescence property of **1**, a simple device was developed and successfully demonstrated potential for rewritable data recording.

2. Experimental

2.1. Regent and materials

All reactions were protected by a dry argon. Intermediate Pt(PhenC≡C$SiMe_3$)Cl_2 was prepared by similar synthetic procedure described in literature [47]. Other reagents were obtained from commercial sources and used as received.

2.2. Synthesis of the complex Pt(PhenC≡C$SiMe_3$)(C≡C-C_6H_4-3-F)$_2$ (**1**)

Intermediate Pt(PhenC≡C$SiMe_3$)Cl_2 (108.5 mg, 0.20 mmol), CuI (1 mg), $^{i}Pr_2NH$ (2 mL), and 1-ethynyl-3-fluorobenzene (60.1 mg, 0.50 mmol) in CH_2Cl_2 (45 mL) were stirred overnight at 30 °C. The pure product was obtained by chromatography on a silica gel column using CH_2Cl_2 as eluent. Yield: 113.6 mg (80%). IR (neat, cm^{-1}): 3067(w), 2957(m), 2898(m), 2163(m), 2115(s), 1605(s), 1572(s), 1482(s), 1430(m), 1347(w), 1255(m), 1242(s), 1162(w), 1136(s), 1113(w), 1071(w), 987(m), 942(m), 897(m), 859(s), 844(s), 827(m), 774(m), 760(m), 709(m), 682(m), 657(m). ESI-MS *m*/*z* calculated for $[M+H]^+$ 710.7, found 710.7. ^{1}H NMR (400 MHz, $^{DMSO\text{-}d}_6$, ppm): δ 9.627 (s, 1H), 9.593 (d, J = 4.0 Hz, 1H), 9.141 (s, 1H), 8.940 (d, J = 6.4 Hz, 1H), 8.190 (dd, J = 22.8, 7.2 Hz, 2H), 8.151 (dd, J = 6.4, 4.0 Hz, 1H), 7.039 (m, 8H), 0.308 (s, 9H). ^{13}C NMR (100 MHz, $CDCl_3$, ppm): δ 163.87, 161.92, 154.05, 151.87, 147.88, 146.58, 139.99, 138.23, 131.15, 130.33, 129.55, 129.54, 129.48, 129.47, 128.55, 128.49, 127.53, 126.46, 119.28, 119.24, 119.11, 119.06, 113.36, 113.33, 113.19, 113.16, 104.34, 99.77, 86.91, 86.41, 0.42. Elem. Anal.: $C_{33}H_{24}F_2N_2PtSi$ (%) Calcd for: C, 55.85; H, 3.41; N, 3.95. Found (%): C, 55.84; H, 3.47; N, 3.97. UV/Vis (CH_2Cl_2) λ_{max} nm (log ε): 439 (3.772), 414(3.843), 331 (4.336), 307 (4.579), 281 (4.773), 242 (4.664).

2.3. Measurements

Nicolet 6700 FT-IR Spectrometer provided the Infrared (IR) spectra and Bruker Advance II (400 MHz) spectrometer determined the ^{1}H NMR and ^{13}C NMR spectra. The photo-physical properties were recorded on the Perkin-Elmer Lambda 25 UV–vis spectrometer and the Edinburgh analytical instrument (F910 fluorescence spectrometer). Thermogravimetric analysis (TGA) was measured under the N_2 atmosphere using a TA-Q50 thermogravimetric analyzer with a heating rate of 5 °C/min. Elemental analysis of C, H and N were carried out on a Perkin-Elmer model 240C elemental analyzer. Electrospray ionization mass spectra (ESI-MS) was provided by Finnigan LCQ mass spectrometer. Powder X-ray diffraction (PXRD) were performed on the D/MAX-2400 with the scan rate of 5°/min.

2.4. X-ray crystallography

Crystals of **1**·$CHCl_3$ and **1**·1/2($ClCH_2CH_2Cl$) were obtained by diffusing petroleum ether onto its chloroform and 1, 2-dichloroethane solution, respectively. The Bruker SMART APEX II CCD area detector system were used to collect the data of crystals. Direct methods was used to solved the structures and all non-hydrogen atoms were refined by a full-matrix least-squares methods procedure on F^2 with anisotropic thermal parameters using the SHELXTL–97 program package [48,49]. The detailed crystallographic data and structure refinement parameters were given in Table S1 of the Supplementary Data.

2.5. Data recording procedures

The functional paper was prepared by coating **1**·$CHCl_3$ onto a piece of common paper such as a filter paper, print paper, or tissue paper. Data input and recording were simultaneously realized by writing the message on the functional paper using a metal cone as the “pen”. Data erasure and paper regeneration can be easily achieved by exposing the paper to $CHCl_3$ vapor within 1 min.

3. Results and discussion

3.1. Preparation and structures

Complex **1** was prepared in high yield by reaction of the

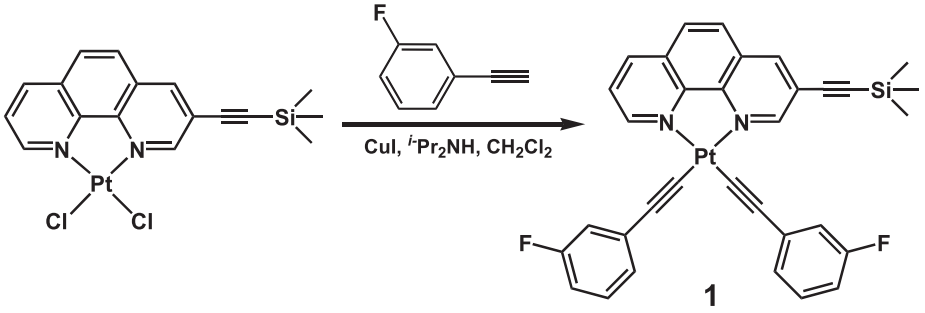

Scheme 1. Synthetic routes of complex **1**.

precursor Pt(PhenC≡CSiMe$_3$)Cl$_2$ with 1-ethynyl-3-fluorobenzene and was fully characterized by NMR spectroscopy, ESI-MS, IR and elemental analysis. Two kinds of solvated single-crystals, the yellow-green **1**·1/2(ClCH$_2$CH$_2$Cl) and the yellow **1**·CHCl$_3$, suitable for structural determination were obtained and their structures were clearly resolved.

The structures of **1**·1/2(ClCH$_2$CH$_2$Cl) and **1**·CHCl$_3$ are shown in Fig. 1, while Table S2 gives their selected bond lengths and angles. In both structures, each Pt center is coordinated by two *N* atoms from phenanthroline ligand and two *C* atoms from two alkynyl auxiliary ligands and adopts the square-planar geometry. The solvated molecules are all located in the space between two acetylene auxiliary ligands and stabilized by forming the strong hydrogen bonds with Pt(II) moieties (Fig. 1 and Table S3). In **1**·1/2(ClCH$_2$CH$_2$Cl), two neighbouring Pt(II) moieties form an antiparallel dimer motif by π(C18≡C19)···π(phen ring) stacking interactions (Fig. 2a). The larger separation (4.375 Å) between Pt atoms in the dimer motif indicates that no metal-metal interaction exists in **1**·1/2(ClCH$_2$CH$_2$Cl). Adjacent dimer motifs along *a* axis are combined with each other and form the one-dimentional (1D) platinum(II) columnar stacking structure through π(C18≡C19)···π(phen ring) stacking interactions (Fig. 2b and Table S3). These platinum(II) columns connect with each other through hydrogen bonds to construct the 3D supramolecular networks (Fig. 2c, Fig. S1 and Table S3).

In **1**·CHCl$_3$, the dimer motif is also formed by neighboring Pt(II) moieties with antiparallel packing pattern through hydrogen bonds (Fig. S2). Due to the severe slide between Pt(II) moieties, no Pt-Pt (4.397 Å) and π···π stacking interactions exists in the dimer motif. Along *a* axis direction, adjacent dimer motifs construct a chain structure which is stabilized by hydrogen bonds (Fig. S3a and Table S3). Meanwhile, the CHCl$_3$ molecules also stacks in a chain structure along *a* axis through Cl···Cl contacts (Fig. S3b and Table S3). Both Pt(II) moiety and solvent molecular chains are arranged alternately to construct the 2D layer (Fig. S3c). Neighbouring 2D layers are combined by hydrogen bonds and construct the 3D supramolecular networks (Fig. S4 and Table S3).

3.2. Photophysical properties

In CH$_2$Cl$_2$ solution, **1** exhibits high-energy absorption bands at about 242, 281, 307, and 331 nm and low-energy bands at *ca.* 414 and 439 nm (Fig. S5 and Table 1). The high energy bands can be assigned to the intraligand ^{1}IL (PhenC≡CSiMe$_3$) charge transfer transition, whereas the low-energy bands most likely arises from a mixture of dπ(Pt) → π*(PhenC≡CSiMe$_3$) ^{1}MLCT and π(C≡CC$_6$H$_4$-3-F) → π*(PhenC≡CSiMe$_3$) ligand-to-ligand charge transfer (^{1}LLCT) transitions according to reported complexes with similar structure [39]. In dilute CH$_2$Cl$_2$ solution, **1** displays a bright yellow luminescence with a broad emission spectra peaked at 569 nm (Fig. S5 and Table 1), resulting from the admixture of ^{3}MLCT and ^{3}LLCT triplet states [47].

In solid state, **1**·1/2(CH$_2$ClCH$_2$Cl) and **1**·CHCl$_3$ display very similar UV–Vis absorption spectra with low-energy absorption at *ca.* 412–506 nm, arising most likely from both ^{1}LLCT and ^{1}MLCT transitions (Fig. 3a). Under irradiation at 350 < λ_{ex} < 460 nm, both **1**·1/2(CH$_2$ClCH$_2$Cl) and **1**·CHCl$_3$ emit a bright green luminescence with emission bands peaked at 514 and 544 nm for **1**·1/2(CH$_2$ClCH$_2$Cl), and 502 and 535 nm for **1**·CHCl$_3$ (Fig. 3b and Table 1), attributing to the admixture of ^{3}MLCT and ^{3}LLCT triplet states. The slight differences in absorption and emission spectra between **1**·1/2(CH$_2$ClCH$_2$Cl) and **1**·CHCl$_3$ are due to the existence of aromatic π···π stacking interactions in **1**·1/2(CH$_2$ClCH$_2$Cl) which can reduce the HOMO-LUMO energy gap [50].

3.3. Thermo-triggered luminescence switching property

Upon heating at 80 °C, the color and luminescence of **1**·1/2(CH$_2$ClCH$_2$Cl) changed gradually from yellow-green to orange and from green to red, respectively [Fig. 4a]. The dynamic variation of luminescence spectra indicated that the original green emission spectra peaked at 514 and 544 nm gradually weakened and finally disappeared, whereas a new broad emission band centered at 656 nm emerged and grew progressively during the heating process [Fig. 4b]. Thermogravimetric analysis (TGA) and PXRD measurement revealed that the final heated sample is a solvent-free species with the crystalline state of a new stacking structure [Figs. S6(a) and S7]. Interestingly, the thermo-triggered luminescence switching behavior of **1**·1/2(CH$_2$ClCH$_2$Cl) are fully reversible because the color, luminescence as well as stacking structure could be restored to the original crystalline state of **1**·1/2(CH$_2$ClCH$_2$Cl) once exposure the heated sample to CH$_2$ClCH$_2$Cl vapor (Fig. S7).

Similarly, **1**·CHCl$_3$ also exhibits reversible thermo-triggered luminescence switching property. Upon heating at 100 °C, both color and luminescence of **1**·CHCl$_3$ changed from green to red with emission wavelength red-shifting from original 502 and 535 nm to 691 nm, corresponding to a thermo-triggered luminescence shift of ca. 156–189 nm (Fig. S8 and Table 1). The heated sample of **1**·CHCl$_3$ is also a solvent-free and crystalline species which can be fully restored to original crystalline **1**·CHCl$_3$ by absorbing CHCl$_3$ vapor [Figs. S6(b) and S8]. It is obviously that the color and luminescence changes of both complexes during the heating-restoring process are caused by structural transformation arising from the desorption/absorption of solvent molecule. Considering the large shifts of

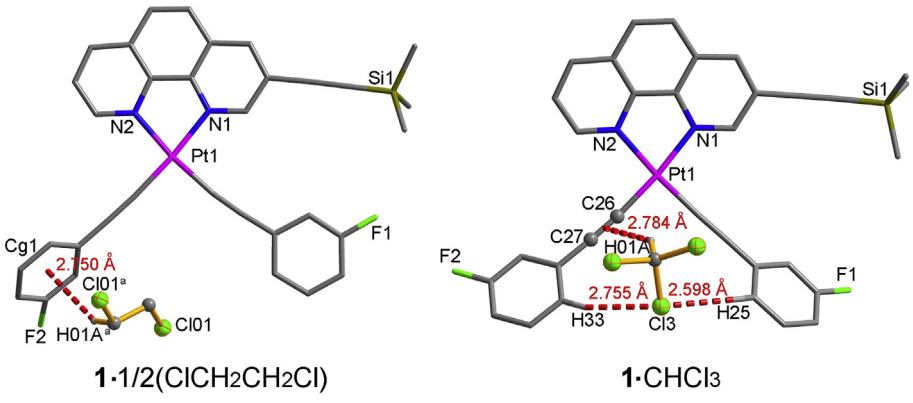

1·1/2(ClCH$_2$CH$_2$Cl) **1**·CHCl$_3$

Fig. 1. Molecular structures of **1**·1/2(ClCH$_2$CH$_2$Cl) and **1**·CHCl$_3$. Hydrogen atoms not involved in hydrogen bonds are omitted for clarity. Symmetry code: a = 1-x, -y, 2-z.

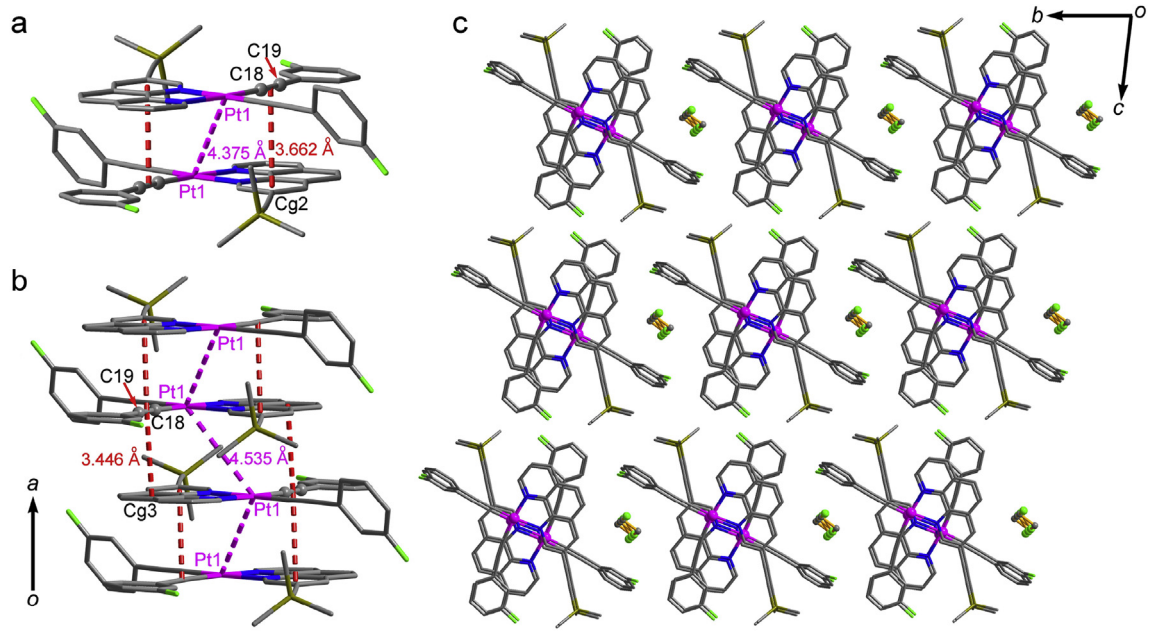

Fig. 2. (a) The structure of a dimer motif formed by two neighbouring Pt(II) moieties, (b) the Pt(II) columnar structure along *a* axis, and the stacking structure of **1**·1/2($ClCH_2CH_2Cl$). Hydrogen atoms are omitted for clarity.

Table 1
Luminescence data of **1** in different states at ambient temperature.

sample	medium	λ_{em} (nm)	τ_{em} (μs)	Φ_{em} (%)
1	CH_2Cl_2 solution	569	0.343	10.72[a]
1·1/2($ClCH_2CH_2Cl$)	crystalline	514, 544	0.374	13.80
	heated	656	0.237	2.51
	ground	702	0.134	0.22
1·$CHCl_3$	crystalline	502, 535	0.489	20.10
	heated	691	0.147	0.56
	ground	702	0.134	0.22

[a] The quantum yield was estimated relative to $[Ru(bpy)_3](PF_6)_2$ in CH_3CN as the standard ($\Phi_{em} = 6.2\%$).

absorption and emission spectra, we can conclude that the mechanism of thermo-triggered luminescence switching property of both complexes is the conversion of excited states from MLCT to MMLCT transitions upon heating [41,44,50].

It should be noted that the heated samples of **1**·1/2(CH_2ClCH_2Cl) and **1**·$CHCl_3$ are all stable species with different stacking structures and photophysical properties. This result provides a direct evidence that the stacking structure of the complexes may influence their responses to external stimulus which is very important for expanding the application fields of luminescent switching materials [6].

3.4. Mechanoluminescence

In addition to the thermo-triggered luminescence switching property, both **1**·1/2($ClCH_2CH_2Cl$) and **1**·$CHCl_3$ also exhibit the mechanoluminescence property. Upon mechanical grinding, the luminescence of them exhibited the dramatic changes from green to red with the emission spectra changing from two vibronic-structured bands to a broad unstructured band centered at 702 nm (Fig. 5 and Fig. S9 and Table 1). The corresponding luminescence response shifts of both complexes to the mechanical

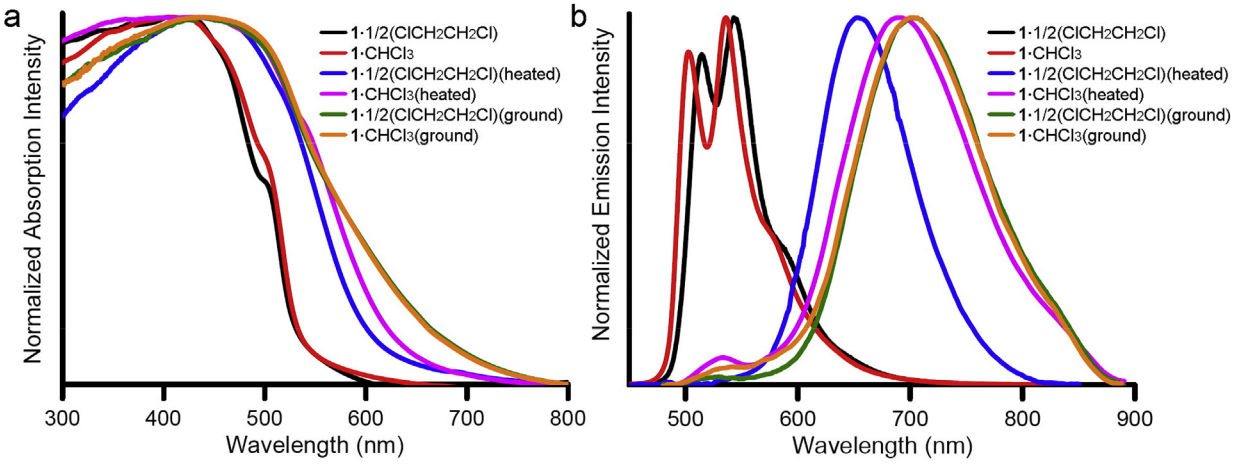

Fig. 3. The UV–Vis absorption (a) and emission spectra (b) of crystalline **1**·1/2($ClCH_2CH_2Cl$) and **1**·$CHCl_3$ in different states.

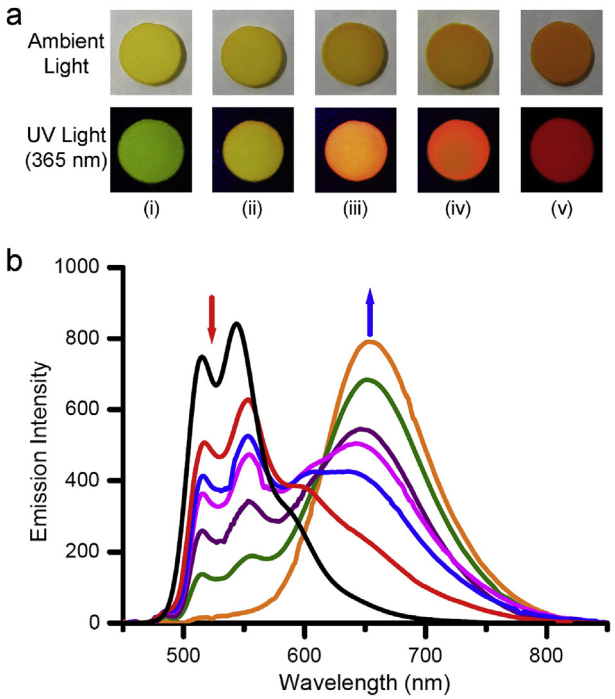

Fig. 4. (a) Photographic images of color and luminescence changes of **1**·1/2($ClCH_2CH_2Cl$) upon heating at 80 °C. (i) heated after 0 min, (ii) heated after 3 min, (iii) heated after 5 min, (iv) heated after 10 min, (v) heated after 20 min. (b) The emission spectral changes of **1**·1/2($ClCH_2CH_2Cl$) during the heating process. (For interpretation of the references to color in this figure legend, the reader is referred to the Web version of this article.)

grinding are *ca.* 158–188 nm and 167–200 nm, respectively. The PXRD and TGA measurements reveal that both red ground samples are in an amorphous phase without containing any solvent molecule (Fig. 5, Fig. S6 and S9). As a strong external stimulus, mechanical grinding can usually destroy all original crystalline structures of the complex into amorphous phase. Therefore, with the same color, luminescence and amorphous phase, it is no doubted that both ground samples are the same product. Interestingly, once either a drop of $ClCH_2CH_2Cl$ or $CHCl_3$ was added or exposed to their vapors, the color, luminescence and PXRD patterns of the ground sample could be converted back to those of crystalline **1**·1/2($ClCH_2CH_2Cl$) or **1**·$CHCl_3$, respectively (Fig. 5 and Fig. S9). The results demonstrate that the mechanoluminescence property of both complexes are fully reversible.

Although mechanical grinding can remove the solvent molecules from the complex, the mechanoluminescence property of **1**·1/2($ClCH_2CH_2Cl$) and **1**·$CHCl_3$ are not due to the desorption of the solvent molecules because emission spectra of the ground samples are more red-shifted than those of heated samples. It is well known that square-planar Pt(II) complex favors formation of dimer or aggregate forms through Pt-Pt contact and/or π-π interactions under the external stimulus [6–8,11,39–41]. Compared with the π-π interaction, the formation of Pt-Pt contact will change the excited states of the complex from MLCT to MMLCT, leading to drastic red-shift (usually larger than 120 nm) of luminescence spectra [6–8,11,41,44,50]. Furthermore, we also found that the emission wavelength of almost all diimine-Pt(II) bisacetylide complexes with Pt-Pt interaction are beyond 650 nm [6–8,11,41,44,50]. Considering the large emission red-shift and long wavelength emission band of ground samples, the reversible mechanoluminescence property of the complexes are most likely caused by interconversion between crystalline and amorphous states as well as the conversions in the lowest energy excited states between MLCT to MMLCT transitions during the mechanical grinding-vapor absorbing processes [6–8,11,41,44,50].

Based on its reversible mechanoluminescence property, complex **1** was successfully used to develop a simple rewritable data recording device. As shown in Fig. 6 and Fig. S10, on a piece of **1**·$CHCl_3$-coated print paper, a metal cone was used as the "pen" to

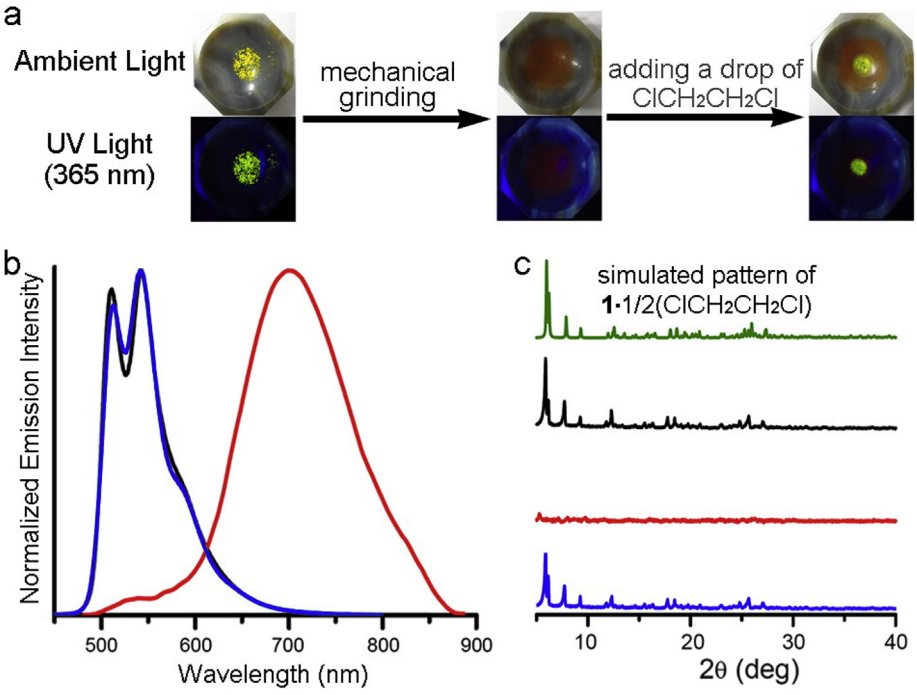

Fig. 5. The reversible mechanoluminescence of **1**·1/2($ClCH_2CH_2Cl$). (a) Photographic images of samples under ambient light and UV light (365 nm) irradiation during the reversible process. (b) Emission spectra and (c) PXRD patterns of unground sample (black line), ground sample (red line), and ground sample with a drop of $ClCH_2CH_2Cl$ added (blue line). (For interpretation of the references to color in this figure legend, the reader is referred to the Web version of this article.)

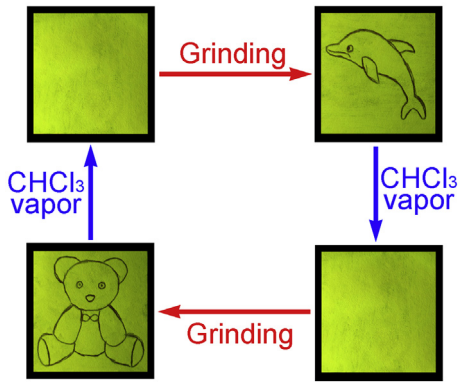

Fig. 6. The practical application of **1**·$CHCl_3$ for rewritable data recording device. All photographs were taken in the UV light (365 nm) with the digital camera.

write the message (the image of a dolphin). The message will be recorded on the paper because the color and luminescence of message changed from yellow to red whereas the background is unchanged. The recorded message can be easily erased upon exposure to $CHCl_3$ vapor and the paper can be used to record other message (the cartoon image of a bear). Furthermore, this device exhibits excellent regeneration and reusability as the luminescence of device has not any change after 21 cycles of writing/erasing process (Fig. S11).

4. Conclusions

In this study, a new dual-stimulus-responsive luminescent platinum(II) complex was designed and synthesized. Two solvated crystals **1**·1/2($ClCH_2CH_2Cl$) and **1**·$CHCl_3$ which stacked in different structures and exhibited bright green luminescence were obtained. Upon heating, their luminescence will gradually changed to red with emission spectra red-shifting to 656 and 691 nm, respectively. Furthermore, they can also be converted to the same red amorphous product with broad unstructured emission band centered at 702 nm under the mechanical grinding. Interestingly, once exposure to $ClCH_2CH_2Cl$ or $CHCl_3$ vapor, the heated and ground samples will be thoroughly converted back to original crystalline **1**·1/2($ClCH_2CH_2Cl$) or **1**·$CHCl_3$, indicating their luminescence switching behaviors are fully reversible. The systematic studies clearly revealed that the thermo- and mechanical-grinding-triggered luminescence switching properties of the complexes are attributed to the interconversions of the lowest energy excited states between MLCT to MMLCT transitions during the heating/grinding-vapor absorbing processes. Importantly, the different heating products of **1**·1/2($ClCH_2CH_2Cl$) and **1**·$CHCl_3$ provided conclusive evidence that the original stacking structure can accurately affect the luminescence switching properties of LSMs. Furthermore, **1**·$CHCl_3$ was successfully used to develop a simple device for rewritable data recording.

Acknowledgements

This work is supported by the National Natural Science Foundation of China (21471024, 21871038).

Appendix A. Supplementary data

Supplementary data to this article can be found online at https://doi.org/10.1016/j.jorganchem.2019.07.004.

References

[1] O.S. Wenger, Chem. Rev. 113 (2013) 3686–3733.
[2] A.J. McConnell, C.S. Wood, P.P. Neelakandan, J.R. Nitschke, Chem. Rev. 115 (2015) 7729–7793.
[3] K.Y. Zhang, S.J. Liu, Q. Zhao, W. Huang, Coord. Chem. Rev. 319 (2016) 180–195.
[4] Z.Q. Guo, S. Nam, S. Park, J. Yoon, Chem. Sci. 3 (2012) 2760–2765.
[5] J.C. Zhang, C. Pan, Y.F. Zhu, L.Z. Zhao, H.W. He, X.F. Liu, J.R. Qiu, Adv. Mater. 30 (2018) 1804644.
[6] J.J. Kang, J. Ni, M.M. Su, Y.Q. Li, J.J. Zhang, H.J. Zhou, Z.N. Chen, ACS Appl. Mater. Interfaces 11 (2019) 13350–13358.
[7] A.K.W. Chan, V.W.W. Yam, Acc. Chem. Res. 51 (2018) 3041–3051.
[8] L.R. Gao, J. Ni, M.M. Su, J.J. Kang, J.J. Zhang, Dyes Pigments 165 (2019) 231–238.
[9] S. Nagai, M. Yamashita, T. Tachikawa, T. Ubukata, M. Asami, S. Ito, J. Mater. Chem. C 7 (2019) 4988–4998.
[10] L. Chen, J.W. Ye, H.P. Wang, M. Pan, S.Y. Yin, Z.W. Wei, L.Y. Zhang, K. Wu, Y.N. Fan, C.Y. Su, Nat. Commun. 8 (2017) 15985.
[11] X. Zhang, B. Li, Z.H. Chen, J. Mater. Chem. 22 (2012) 11427–11441.
[12] X. Li, Y. Xie, B. Song, H.L. Zhang, H. Chen, H. Cai, W. Liu, Y. Tang, Angew. Chem. Int. Ed. 56 (2017) 2689–2693.
[13] J. Wang, S. Chen, X.Y. Cheng, Q. Peng, W.K. Li, Opt. Mater. 86 (2018) 56–61.
[14] M.G. Zhang, J. Wei, Y.N. Zhang, B.L. Bai, F.Y. Chen, H.T. Wang, M. Li, Sens. Actuators, B 273 (2018) 552–558.
[15] Y.Z. Zhang, H.Y. Yang, H.L. Ma, G.F. Bian, Q.G. Zang, J.W. Sun, C. Zhang, Z.F. An, W.Y. Wong, Angew. Chem. Int. Ed. 58 (2019) 8773–8778.
[16] Y. Ma, S.J. Liu, H.R. Yang, Y. Zeng, P.F. She, N.Y. Zhu, C.L. Ho, Q. Zhao, W. Huang, W.Y. Wong, Inorg. Chem. 56 (2017) 2409–2416.
[17] J. Wang, S. Chen, H. Liu, W.K. Li, J. Rare Earths 36 (2018) 733–738.
[18] W. Li, W. Deng, X.Q. Fan, F.J. Chun, M.L. Xie, C. Luo, S.Y. Yang, H. Osman, C.Q. Liu, X.T. Zheng, W.Q. Yang, Ceram. Int. 44 (2018) 18123–18128.
[19] X. Zhang, N.Y. Xu, Q. Ruan, D.Q. Lu, Y.H. Yang, R. Hu, RSC Adv. 8 (2018) 5714–5720.
[20] Y. Chen, L.B. Li, L.S. Gong, T.Y. Zhou, J.B. Liu, Adv. Funct. Mater. 29 (2019) 1806945.
[21] Y.N. Huang, Q.B. Xiao, J. Wang, Y.L. Xi, F.J. Li, Y.M. Feng, L.Y. Shi, H.Z. Lin, J. Lumin. 173 (2016) 66–72.
[22] Q. Chai, J. Wei, B.L. Bai, H.T. Wang, M. Li, Dyes Pigments 152 (2018) 93–99.
[23] Z.B. Sun, J.K. Liu, D.F. Yuan, Z.H. Zhao, X.Z. Zhu, D.H. Liu, Q. Peng, C.H. Zhao, Angew. Chem. Int. Ed. 58 (2018) 4840–4846.
[24] J.F. Li, C.L. Yang, X.L. Peng, Y. Chen, Q. Qi, X.Y. Luo, W.Y. Lai, W. Huang, J. Mater. Chem. C 6 (2018) 19–28.
[25] Z.H. Sun, Q.G. Zang, Q. Luo, C.Y. Lv, F. Cao, Q.B. Song, R.Y. Zhao, Y.J. Zhang, W.Y. Wong, Chem. Commun. 55 (2019) 4735–4738.
[26] E. Cariati, E. Lucenti, C. Botta, U. Giovanella, D. Marinottoc, S. Righetto, Coord. Chem. Rev. 306 (2016) 566–614.
[27] S.K.L. Sui, C.Y.S. Chung, C.W.W. Yan, J. Organomet. Chem. 845 (2017) 177–188.
[28] A. Kobayashi, N. Yamamoto, Y. Shigeta, M. Yoshida, M. Kato, Dalton Trans. 47 (2018) 1548–1556.
[29] S.K. Sheet, B. Sen, S. Khatua, Inorg. Chem. 58 (2019) 3635–3645.
[30] H.V. Miyagishi, T. Tamaki, H. Masai, J. Terao, Molecules 24 (2019) 1301.
[31] H. Masai, J. Terao, Polym. J. 49 (2017) 805–814.
[32] S. Sano, T. Yuuki, T. Hyakutake, K. Morita, H. Sakaue, S. Arai, H. Matsumoto, T. Michinobu, Sens. Actuators, B 255 (2018) 1960–1966.
[33] W.Y. Wong, P.D. Harvey, Macromol. Rapid Commun. 31 (2010) 671–713.
[34] C.L. Ho, Z.Q. Yu, W.Y. Wong, Chem. Soc. Rev. 45 (2016) 5264–5295.
[35] L.L. Xu, C.L. Ho, L. Liu, W.Y. Wong, Coord. Chem. Rev. 373 (2018) 233–257.
[36] W.Y. Wong, C.L. Ho, Coord. Chem. Rev. 250 (2006) 2627–2690.
[37] J. Zhang, L.L. Xu, C.L. Ho, W.Y. Wong, Top. Curr. Chem. 375 (2017) 77.
[38] Q.Y. Wan, W.P. To, C. Yang, C.M. Che, Angew. Chem. Int. Ed. 57 (2018) 3089–3093.
[39] H.L.K. Fu, C. Po, S.Y.L. Leung, V.W.W. Yam, ACS Appl. Mater. Interfaces 9 (2017) 2786–2795.
[40] F.K.W. Kong, A.K.W. Chan, M. Ng, K.H. Low, V.W.W. Yam, Angew. Chem. Int. Ed. 129 (2017) 15299–15303.
[41] J. Ni, X. Zhang, Y.H. Wu, L.Y. Zhang, Z.N. Chen, Chem. Eur J. 17 (2011) 1171–1183.
[42] B. Jiang, J. Zhang, J.Q. Ma, W. Zheng, L.J. Chen, B. Sun, C. Li, B.W. Hu, H.W. Tan, X.P. Li, H.B. Yang, J. Am. Chem. Soc. 138 (2016) 738–741.
[43] A.L. Han, P.W. Du, Z.J. Sun, H.T. Wu, H.X. Jia, R. Zhang, Z.N. Liang, R. Cao, R. Eisenberg, Inorg. Chem. 53 (2014) 3338–3344.
[44] J.J. Kang, X.X. Zhang, H.J. Zhou, X.Q. Gai, T. Jia, L. Xu, J.J. Zhang, Y.Q. Li, J. Ni, Inorg. Chem. 55 (2016) 10208–10217.
[45] A. Kobayashi, M. Kato, Eur. J. Inorg. Chem. (2014) 4469–4483.
[46] J.L.L. Tsai, T.T. Zou, J. Liu, T.F. Chen, A.O.Y. Chan, C. Yang, C.N. Loka, C.M. Che, Chem. Sci. 6 (2015) 3823–3830.
[47] J. Ni, J.J. Kang, H.H. Wang, X.Q. Gai, X.X. Zhang, T. Jia, L. Xu, Y.Z. Pan, J.J. Zhang, RSC Adv. 5 (2015) 65613–65617.
[48] G.M. Sheldrick, SHELXS-97, Program for X-Ray Crystal Structure Determination, University of Gottingen, Germany, 1997.
[49] G.M. Sheldrick, SHELXL-97, Program for X-Ray Crystal Structure Refinement, University of Gottingen, Germany, 1997.
[50] J. Ni, L.Y. Zhang, H.M. Wen, Z.N. Chen, Chem. Commun. (2009) 3801–3803.